EurJIC European Journal of Inorganic Chemistry
ChemPubSoc Europe
FULL PAPER

DOI:10.1002/ejic.201402924

Structural Diversity in Sterically Demanding Diiminophosphinato Alkali Metal Complexes

Andrew L. Hawley[a] and Andreas Stasch*[a]

Keywords: Alkali metals / Chelates / Phosphanes / Ligand design / Steric hindrance

We have prepared the new aminophosphine $Ph_2PNHMes$ **2** [Mes = mesityl (2,4,6-$Me_3C_6H_2$)], and the aminoiminophosphorane $Ph_2P(=NMes)NHMes$ **4** (^{Mes}LH), and obtained the new alkali metal complexes [($^{Dip}LLi)_2$] **5** [$^{Dip}L = Ph_2P(NDip)_2$, Dip = 2,6-*i*$Pr_2C_6H_3$], [($^{Mes}LLi)_2$] **6**, [(^{Dip}L)($^{DipN2}L$)Li_2] **7** [$^{DipN2}L = Ph_2P(NDip)(N_3Dip)$], [($^{DipN2}L)_2Li_2$] **8**, [$^{Dip}LLi(THF)$] **9**, [$^{Dip}LLi(THF)_2$] **10**, [($^{Dip}LNa)_2$] **11**, [($^{Mes}LNa)_n$] **12**, [$^{Dip}LNa(THF)_2$] **13**, [{$^{Mes}LNa(THF)$}$_2$] **14** and [$^{Mes}LK$] **16** by deprotonation of their respective ligand precursors with standard strong alkali metal bases in various solvents. The crystal structures of **2**, **4**–**6**, **7**·**8**, **9**–**14**, and **16** are reported. The different coordination modes in their solid-state structures are discussed and generally compared to the solution behavior of those species.

Introduction

N,*N*′-Chelating and sterically demanding ligands such as β-diketiminates,[1] amidinates, guanidinates and related systems,[2] as well as diazabutadien(edi)ides and similar species[3] have been employed for a wide variety of metal complexes and chemical applications. This includes the stabilization of an impressive array of unusual low-oxidation-state complexes.[4] Related iminophosphorane-based ligands that feature fragments with the general formula $R_3P{=}NR'$ (R, R′ = alkyl, aryl, silyl, amido and so forth) form related ligand systems of similar overall geometry, plus they have the additional advantage of central ^{31}P nuclei for facile ^{31}P NMR spectroscopic studies.[5] These ligands have, however, been employed for low-oxidation-state chemistry to a far lesser extent than CN-based systems.

We have previously used a sterically demanding diiminophosphinate ligand for the stabilization of low-oxidation-state metal complexes and reported metal–metal-bonded dimeric metal(I) complexes of magnesium[6] and zinc[7] (see Scheme 1). These studies have also revealed different properties of the diiminophosphinates relative to related ligands with CN-based backbones. In addition, diiminophosphinate complexes have been prepared with metals from all parts of the periodic table and some sterically demanding ones have successfully been employed in heteroleptic transition-metal[8] or lanthanoid[9] complexes for alkene oligomerizations and polymerizations. Here we report on the synthesis of a new diiminophosphinate ligand and a series of alkali metal complexes that are of interest as convenient starting materials for salt metathesis chemistry,[7] plus we anticipated a rich structural chemistry owing to their flexible properties especially in complexes with electropositive metals.

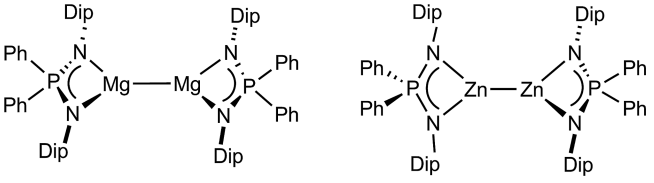

Scheme 1. Diiminophosphinato metal(I) dimers of Mg and Zn (Dip = 2,6-*i*$Pr_2C_6H_3$).

Results and Discussion

Compound Syntheses

The predominantly employed strategies for obtaining diiminophosphinates with a central phosphorane (P^V) centre and related species follow two main routes: a Staudinger pathway that uses an organic azide to oxidize a P^{III} compound, and the Kirsanov route, which substitutes P–X bonds (X = Cl, Br) in a P^V compound by using amines to generate P^V–N compounds.[5] The P^V species in the latter route can be obtained by adding Cl_2 or Br_2 to a suitable P^{III} precursor. We have previously used a Staudinger-based synthesis to obtain the ligand used for the stabilization of the metal(I) dimers [($^{Dip}LM)_2$] (M = Mg, Zn; Scheme 1).[6,7]

Treating chlorodiphenylphosphine with one equivalent of the lithiated aniline $ArNH_2$ [Ar = Dip (2,6-*i*$Pr_2C_6H_3$) or Mes (mesityl, 2,4,6-$Me_3C_6H_2$)] afforded the aminophosphines (phosphinoamines)[10] Ph_2PNHAr (Ar = Dip **1** or Mes **2**) as previously reported for **1**,[11] in good yield (see

[a] School of Chemistry, Monash University,
PO Box 23, Melbourne, Victoria 3800, Australia
E-mail: Andreas.Stasch@monash.edu
http://monash.edu/science/about/schools/chemistry/staff/stasch/

Scheme 2). Further reaction of **1** or **2** in a Staudinger reaction[12] with ArN_3 (Ar = Dip or Mes) afforded the aminoiminophosphoranes $Ph_2P(=NAr)NHAr$ (Ar = Dip **3**[7] or Mes **4**, respectively).

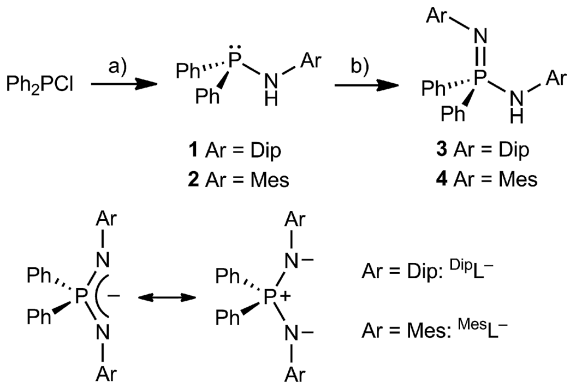

Scheme 2. Synthesis of **1**–**4** and mesomeric forms for diiminophosphinate ligands: (a) LiNHAr (Ar = Dip or Mes), Et_2O; (b) ArN_3, toluene.

Deprotonation of the aminoiminophosphoranes **3** and **4** can conveniently be achieved with standard organometallic or metal amide bases in a range of hydrocarbon or ether solvents. A series of group 1 complexes of related diiminophosphinates have been reported in the literature and were obtained by similar routes.[7,13]

Metallation to the alkali metal complexes of ^{Dip}L and ^{Mes}L here can both be achieved in situ for direct further reactions, or the resulting complexes can be isolated and stored under inert conditions; see Scheme 3 for a simplified synthesis and isolated complexes, and see below for structural studies. Lithiation of **3** and **4** in hexane with *n*-butyllithium afforded the dimeric homoleptic complexes [(^{Dip}LLi)$_2$] **5** and [(^{Mes}LLi)$_2$] **6**, respectively, which can be isolated as colourless, crystalline solids. In some cases in the synthesis of **5**, later crops afforded small amounts of the co-crystallized byproducts [(^{Dip}L)(^{DipN2}L)Li$_2$] **7** and [(^{DipN2}L)$_2$Li$_2$] **8** in a 1:1 ratio. Separation of these latter two compounds so far failed, and only co-crystallized material **7·8** was obtained. We further isolated the THF adducts [^{Dip}LLi(THF)] **9** and [^{Dip}LLi(THF)$_2$] **10** from lithiations in *n*-hexane/THF mixtures or by THF addition to the homoleptic species [(^{Dip}LLi)$_2$] **5**. Sodium and potassium complexes of ^{Dip}L and ^{Mes}L can conveniently be prepared by treating the aminoiminophosphoranes **3** and **4** with [M{N(SiMe$_3$)$_2$}] (M = Na, K) to afford the solvent-free homoleptic sodium complexes [(^{Dip}LNa)$_2$] **11** or [(^{Mes}LNa)$_n$] **12**, the latter of undetermined structure, as well as their isolated THF adducts [^{Dip}LNa(THF)$_2$] **13** or [{^{Mes}LNa(THF)}$_2$] **14** after THF addition, or the respective potassium complexes [^{Dip}LK] **15** and [^{Mes}LK] **16**, respectively; the former was described previously by us.[7] It is also worth noting that alkali metal complexes such as [(^{Dip}LNa)$_2$] **11** and [^{Dip}LK] **15** were obtained as the main products of reduction reactions of [(^{Dip}LMX)$_2$] complexes (M = Mg, Zn; X = halide) using sodium or potassium metal when targeting the aforementioned metal(I) dimers [(^{Dip}LM)$_2$]. The success of isolating the dimeric metal(I) compounds was only achieved using a specialized β-diketiminato magnesium(I) dimer[4a,4c] as a reducing agent.[6,7]

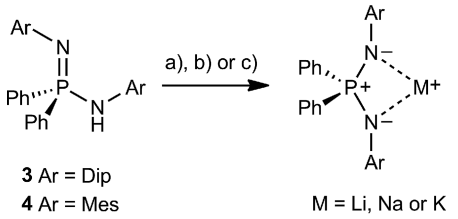

[(^{Dip}LLi)$_2$] **5**, [(^{Mes}LLi)$_2$] **6**, [^{Dip}LLi(THF)] **9**, [^{Dip}LLi(THF)$_2$] **10**, [(^{Dip}LNa)$_2$] **11**, [(^{Mes}LNa)$_n$] **12**, [^{Dip}LNa(THF)$_2$] **13**, [{^{Mes}LNa(THF)}$_2$] **14**, [^{Dip}LK] **15**, [^{Mes}LK] **16**

Scheme 3. Metallation of **3** and **4** and the alkali metal complexes **5**, **6** and **9**–**16**: (a) *n*BuLi, *n*-hexane and/or THF; (b) [Na{N(SiMe$_3$)$_2$}], toluene or *n*-hexane/THF; and (c) [K{N(SiMe$_3$)$_2$}], toluene.

The formation of the phosphazide[14] complexes [(^{Dip}L)(^{DipN2}L)Li$_2$] **7** and [(^{DipN2}L)$_2$Li$_2$] **8** can be explained by an incomplete N_2 elimination in the Staudinger reaction leading to **3** (see Scheme 4). Gas evolution in the synthesis of **3** (and **4**) is already evident at very low temperatures, but very minor impurities can be found in some preparations of **3**, as judged by $^{31}P\{^1H\}$ NMR spectroscopy, which caused the formation of [(^{Dip}L)(^{DipN2}L)Li$_2$] **7** and [(^{DipN2}L)$_2$Li$_2$] **8**. These minor impurities do not easily convert to **3** upon standing at room temperature over prolonged time or at elevated temperatures, although they do appear to slowly diminish after prolonged time at elevated temperatures. The impurities are only evident by several very small $^{31}P\{^1H\}$ NMR resonances +/–0.5 ppm around the base of the singlet at δ = –13.5 ppm in $CDCl_3$ and the concentrations are too low to extract information from ^1H NMR spectroscopy of those samples of **3**. The phosphazide intermediate **A** (see Scheme 4), for which several *E*/*Z* isomers can be considered, is believed to undergo facile N_2 elimination to **3** by means of a cyclic intermediate. This N_2 elimination, however, is likely hindered in the phosphazide tautomers **B** and **C**. Tautomer **C** carries a hydrogen atom on the N_2 fragment that is to be eliminated, and tautomer **B** likely requires H migration before a bond can form between the P atom and the N-Dip moiety. Several *E*/*Z* isomers for all tautomers have to be considered, and the equilibria that exist between them in solution can prevent a suitable *cis*-type isomer[15] of **A** from forming in significant quantities and eliminating N_2. The stability of the isomers might depend on the steric bulk of the attached aryl substituents, and it is worth mentioning that stable phosphazide products as precursors for **3** and **4** have so far only been forthcoming for Dip compounds (i.e., the synthesis of **7·8**) in our laboratories and not for Mes derivatives. Despite their low concentrations in later crops of ^{Dip}LH **3**, all isomers **A**–**C** are expected to be deprotonated to the new ligand ^{DipN2}L$^-$, which is shown in its dominant mesomeric form in Scheme 4. The high solubility of ^{Dip}LH **3** even in

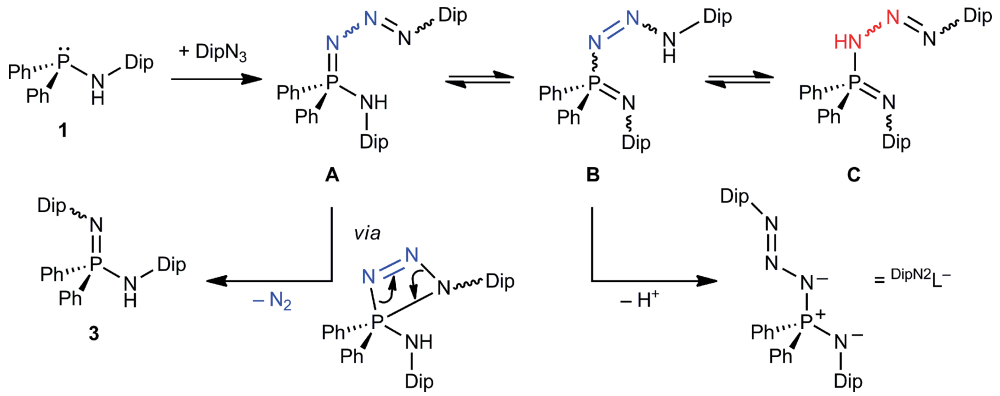

Scheme 4. Staudinger reaction, phosphazide tautomers **A**–**C**, and ligand $^{DipN2}L^{-}$.

aliphatic solvents such as *n*-hexane or *n*-pentane means that recrystallizations have to be performed from concentrated solutions, thereby potentially resulting in impure material, and that repeated recrystallizations lead to a significant loss in yield. In contrast, ^{Mes}LH **4** shows a lower solubility in hydrocarbon solvents, a higher tendency to crystallize and is readily isolated from the respective reaction mixture in better yields than with **3**. Prolonged heating of **7·8** (e.g., 90 °C for one day in deuterated benzene) does not lead to any significant N_2 elimination and formation of **5**, though some minor changes to the heated mixture have been observed by NMR spectroscopy. This stability is likely caused by the inability of the ^{DipN2}Li unit to form the required P–N contact in a four-membered ring transition state in the correct geometry,[15] as represented in Scheme 4, owing to coordination of the nitrogen atoms to the Li cations (see below for the structure of **7·8**).

Structural Studies

Structural representations of the new compounds reported in this paper are shown in Figures 1–8 and selected metrical parameters are summarized in Table 1, whilst crystallographic data is given in Table 2. The overall molecular structure of Ph_2PNHMes **2** (Figure 1, left), including metrical parameters, resembles that of the Dip derivative **1**[11] and related aminophosphines.[10] Two crystal structures for the aminoiminophosphorane Ph_2P(=NMes)NHMes **4** were determined (Figure 1, compound **4′** middle and **4′′** right) that show similar bond lengths around the P^V centre between them, including one short P=N bond (ca. 1.55 Å) and a longer P–N single bond (average ca. 1.67 Å), and are comparable to one polymorph determined for Ph_2P(=NDip)NHDip **3**.[7] The packing and orientation of the substituents around the tetrahedral P centre are dissimilar for the monoclinic (**4′**) and the triclinic (**4′′**) polymorph, which is also reflected in the significantly different N–P–N angles (**4′** larger by 13°), C–P–C angles (**4′′** larger by 4°) and a larger N···N separation for **4′** by approximately 0.2 Å. The differences in the geometries of **4′** and **4′′** cannot be expressed as simple explicit isomers, such as *E*/*Z* isomers.

The molecular structures of $[(^{Dip}LLi)_2]\cdot C_6H_{14}$ (**5**·C_6H_{14}) and $[(^{Mes}LLi)_2]\cdot C_6H_6$ (**6**·C_6H_6) are shown in Figure 2. Owing to the different steric profiles of the ligands, the dimeric units show different Li coordination between them. In **5**·C_6H_{14}, the two Li positions are disordered and the minor Li positions (not shown in Figure 2) adopt a very similar coordination geometry between the two diiminophosphinate ligands relative to the main Li positions. Li1 acts as a bridge between two N–C(Dip) bonds of different diiminophosphinate ligands and shows a short contact to one isopropyl group with a Li1···H(methine) interaction of ap-

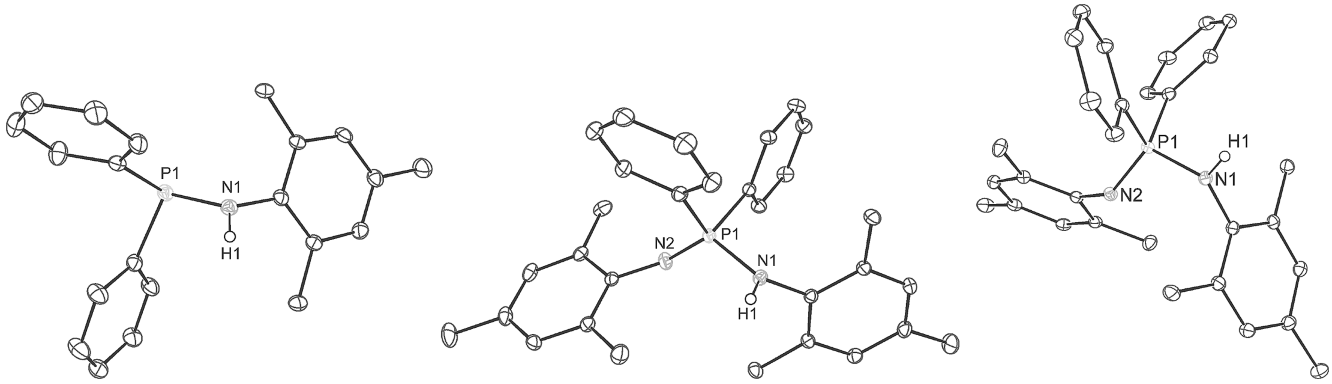

Figure 1. Molecular structures of compound **2** (left), **4′** (middle) and **4′′** (right) (30% probability thermal ellipsoids). Hydrogen atoms except for H1 are omitted for clarity.

Table 1. Selected bond lengths [Å] and angles [°].

Compound	**2**	**4** (**4′**)	**4** (**4′′**)	**5**·C_6H_{14}	**6**·C_6H_6	**7**·**8**·C_6H_{14}	**9**
P–N	P1–N1 1.701(2)	P1–N1 1.6768(10) P1–N2 1.5451(10)	P1–N1 1.6567(15) P1–N2 1.5460(11)	P1–N1 1.5961(14) P1–N2 1.6116(14) P2–N3 1.5901(14) P2–N4 1.6109(15)	P1–N1 1.5870(12) P1–N2 1.6146(12)	P1–N2 1.595(3) P1–N1 1.617(3) P2–N3 1.584(3) P2–N4 1.664(3) P3–N7 1.580(3) P3–N8 1.661(3) P4–N11 1.580(4) P4–N12 1.645(4)	P1–N1 1.5917(14) P1–N2 1.5898(13) P2–N4 1.5836(14) P2–N3 1.6028(14)
M–N	–	–	–	N1–Li2A 1.925(9) N1–Li1 1.933(5) Li1–N4 1.950(5) N2–Li1A 1.963(9) N2–Li2 1.971(4) N2–Li2A 2.423(9) Li2–N3 1.943(4) Li2–N4 2.406(5) N3–Li1A 1.953(9) N4–Li2A 1.963(9)	N1–Li1 1.967(3) Li1–N4 1.998(3) Li1–N2 2.073(3) N2–Li2 2.002(3) Li2–N3 1.951(3) Li2–N4 2.119(3)	N1–Li2 1.970(6) N1–Li1 2.339(6) Li1–N2 1.927(6) Li1–N6 2.061(6) Li1–N4 2.182(6) Li1–N5 2.537(6) Li2–N3 1.938(6) Li2–N4 2.209(6) Li3–N7 1.959(7) Li3–N14 2.059(7) Li3–N12 2.117(7) Li3–N8 2.226(7) Li3–N13 2.524(7) Li3–Li4 2.663(10) Li4–N11 1.935(8) Li4–N10 2.020(9) Li4–N8 2.159(8) Li4–N12 2.206(8) Li4–N9 2.528(8)	N1–Li1 1.968(3) Li1–N2 1.962(3) Li2–N3 1.970(3) Li2–N4 2.010(3)
M–O	–	–	–	–	–	–	Li1–O1A 1.835(12) (63% part) Li1–O1 1.95(2) (37% part) O2–Li2 1.859(3)
M···C	–	–	–	Li1–C13 2.443(5) Li1–C61 2.478(5) (*ipso*-N4) Li1–C62 2.478(5) (*ortho*-N4) Li1–C67 2.691(5) (methine-N4, with H67 contact: 2.070) Li1A–C25 2.620(5) (*ipso*-N2) Li1A–C49 2.430(5) (*ipso*-N3) Li1A–C31 2.688(5) (methine-N2, with H31 contact: 2.015)	Li contacts to *ipso*-C Li1–C52 2.701(3) Li2–C22 2.518(3)	Li2–C13 2.585(7)	no short intra- or intermolecular Li···C contacts found
N···N/N–N	–	N1···N2 2.803	N1···N2 2.593	N1···N2 2.570 N3···N4 2.552	N1···N2 2.495 N1···N2 2.518	N4–N5 1.356(4) N5–N6 1.278(4) N8–N9 1.362(4) N9–N10 1.264(4) N12–N13 1.316(5) N13–N14 1.231(5) N1···N2 2.534 N3···N4 2.512 N4···N6 2.178 N7···N8 2.516 N8···N10 2.165 N11···N12 2.500 N12···N14 2.099	N1···N2 2.479 N3···N4 2.517

Table 1. (*Continued*)

Compound	2	4 (4′)	4 (4′′)	5·C_6H_{14}	6·C_6H_6	7·8·C_6H_{14}	9
N–P–N	–	N2–P1–N1 120.87(5)	N2–P1–N1 108.09(6)	N1–P1–N2 106.49(7) N3–P2–N4 105.75(7)	N1–P1–N2 102.37(6) N3–P2–N4 103.46(6)	N2–P1–N1 104.30(14) N3–P2–N4 101.31(13) N7–P3–N8 101.83(15) N11–P4–N12 101.76(18)	N2–P1–N1 102.38(7) N4–P2–N3 104.38(7)
C–P–C	C7–P1–C1 101.30(10)	C1–P1–C7 108.19(5)	C7–P1–C1 103.55(6)	C7–P1–C1 101.72(7) C43–P2–C37 100.85(7)	C7–P1–C1 103.53(7) C37–P2–C31 101.92(6)	C7–P1–C1 103.10(16) C43–P2–C37 104.65(15) C79–P3–C73 106.11(17) C115–P4–C109 102.4(2)	C7–P1–C1 101.91(8) C47–P2–C41 100.69(7)
N–M–N	–	–	–	N1–Li1–N4 139.1(3) N3–Li2–N2 139.6(3) N3–Li2–N4 70.96(15) N2–Li2–N4 137.7(2) N3–Li2–P1 135.2(2) N3–Li1A–N2 139.5(5) N1–Li2A–N4 138.7(5) N1–Li2A–N2 71.4(3) N4–Li2A–N2 137.1(5)	N1–Li1–N2 76.20(10)	N2–Li1–N1 72.2(2) N3–Li2–N4 74.2(2) N7–Li3–N8 73.6(2) N11–Li4–N12 74.0(3)	N2–Li1–N1 78.20(12) N3–Li2–N4 78.45(11)
M···M	–	–	–	Li1···Li2 2.739 Li1A···Li2A 2.746 (65:35 parts for two Li)	Li1···Li2 2.478(3)	Li1···Li2 2.607(8) Li3··Li4 2.663(10)	–

proximately 2.07 Å. Related coordination of two Li cations between two sterically demanding ligands of similar overall structure has been observed for amidinates and guanidinates that bear N-Dip substituents.[16] Each Li cation in complex **6**·C_6H_6 coordinates to one diiminophosphinate in an *N*,*N*′-chelating fashion whilst only coordinating to one nitrogen centre of the second ligand and further results in relatively short Li···C(*ipso*-Dip) contacts (see Table 1). This yields a folded *cis*-ladder motif of three fused four-membered rings with a central N_2Li_2 diamond at its base.

The byproduct [(^{Dip}L)(^{DipN2}L)Li_2]·[(^{DipN2}L)$_2Li_2$]·C_6H_{14} (**7**·**8**·C_6H_{14}) shows the full independent molecules [(^{Dip}L)(^{DipN2}L)Li_2] **7** and [(^{DipN2}L)$_2Li_2$] **8** in the asymmetric unit (see Figure 3). In **7**, Li1 is *N*,*N*′-chelated by the diiminophosphinate of P1 and *N*,*N*′-chelated by the phosphazido N_3 chain of the ^{DipN2}L ligand of P2. Li2 is coordinated in a similar fashion to the Li cations in **6** as it is *N*,*N*′-chelated by the ^{DipN2}L ligand of P2 and only coordinated to N1 of the ^{Dip}L ligand, plus it has a relatively short Li···C(*ipso*-Dip) contact. In [(^{DipN2}L)$_2Li_2$] **8**, each Li centre is bridged between the two ^{DipN2}L ligands by being *N*,*N*′-chelated to an NPN fragment and *N*,*N*′-chelated to the N_3 chain of the second ligand.[17] The four-coordinate Li environments are not in a distorted tetrahedral geometry but rather tend towards planar coordination, likely on account of the steric influences of the involved Dip groups. The N–N and P–N bond lengths in the ^{DipN2}L ligand suggest a dominant charge distribution as drawn for the ligand in Scheme 4 with an N=N double bond.

In the crystal structure of [^{Dip}LLi(THF)] **9**, two independent molecules are found; the THF ligands of both molecules are disordered and only the main contributions are shown in Figure 4. The first molecule (**9**′; Figure 4, left) shows a distorted three-coordinate Li centre that is *N*,*N*′-chelated to the diiminophosphinate ligand and shows coordination to one disordered terminal THF molecule with a P1···Li1–O1/O1A angle of approximately 160–167°. In the second molecule (**9**′′; Figure 4, middle), the THF ligand is significantly displaced from both the least-squares NPNLi plane and a plane orthogonal to that bisecting the P···Li vector, which results in a very distorted three-coordinate Li environment with a P2···Li2–O2 angle of 141.3°. This is likely caused by packing effects and two molecules of **9**′′ are arranged in a dimeric aggregate although they show no significant intermolecular contacts between them. The crystal structure of [^{Dip}LLi(THF)$_2$] **10** (Figure 4, right) resembles a typical four-coordinate structural type with an *N*,*N*′-chelating diiminophosphinate, as has been found for most previously described related diiminophosphinato lithium complexes.[13] The Li–N bonds in **10** are, as expected,

Table 1. (continued).

Compound	**10**	**11**·4C_6H_6	**11**	**13**	**14**·0.5C_6H_6	**16** (**16′**)	**16** (**16′′**)
P–N	P1–N1 1.5836(12) P1–N2 1.5955(12)	P1–N1 1.5875(12) P1–N2 1.5923(12)	P1–N1 1.593(3) P1–N2 1.590(3)	P1–N1 1.584(3) P1–N2 1.579(3)	P1–N1 1.5872(18) P1–N2 1.5978(18) P2–N3 1.5997(17) P2–N4 1.6077(17)	P1–N1 1.5775(14) P1–N2 1.5982(14)	P1–N1 1.5735(14) P1–N2 1.5945(15)
M–N	N1–Li1 2.089(3) Li1–N2 2.039(3)	Na1–N1 2.4837(13) Na1–N2 2.3308(13)	Na1–N1 2.455(4) Na1–N2 2.292(4)	Na1–N1 2.362(3), Na1–N2 2.423(4)	Na1–N2′ 2.3272(19) Na1–N1 2.3456(19) Na2–N3 2.331(2) Na2–N4′ 2.4047(19) Na2–N4 2.684(2) N2–Na1′ 2.3272(19) N4–Na2′ 2.4047(19)	K1–N1 2.7348(14) K1–N2′ 2.7211(13)	K1–N1 2.7171(17) K1–N2′ 2.7197(15)
M–O	O1–Li1 1.975(3) Li1–O2 1.976(3)	–	–	Na1–O1 2.256(4) Na1–O2 2.259(7) Na1–O2A 2.528(11)	Na1–O1 2.273(2) Na2–O2 2.3029(19)	–	–
M···C	–	Na1–C17′ 2.8657(17) Na1–C16′ 2.8770(17) Na1–C15′ 2.8901(17) Na1–C18′ 2.9094(15) Na1–C14′ 2.9132(15) Na1–C13′ 2.9176(15) Na1···$C_{centroid}$ 2.534	Na1–C15′ 2.756(5) Na1–C16′ 2.780(5) Na1–C14′ 2.817(5) Na1–C17′ 2.877(5) Na1–C13′ 2.879(4) Na1–C18′ 2.943(5) Na1···$C_{centroid}$ 2.474	–	Na1–C13 2.887(2) C21–Na1′ 2.980(4) (methyl group, shortest contact H21C, 2.489; H21B 2.618) C22–Na1′ 2.994(2) Na2–C56′ 2.819(2) Na2–C62 2.878(8) (methyl group, shortest contact H62C, 2.379; H62B 2.546)	K1–C13(*ipso*-N1) 3.041 K1–C18(*ortho*-N1) 3.343 K1–C21(methyl-N1) 3.616 (shortest H21B 2.987) K1–C22(*ipso*-N2) 3.468 K1–C23(*ortho*-N2) 3.100 K1–C24(*meta*-N2) 3.221 K1–C22(*ipso*-N2′) 3.428	K1–C13(*ipso*-N1) 3.136 K1–C18(*ortho*-N1) 3.374 K1–C21(methyl-N1) 3.473 (shortest H21B 2.774) K1–C22(*ipso*-N2) 3.384 K1–C23(*ortho*-N2) 3.132 K1–C24(*meta*-N2) 3.228 K1–C22(*ipso*-N2′) 3.518
N···N/N–N	N1···N2 2.510	N1···N2 2.541	N1···N2 2.542	N1···N2 2.566	N1···N2 2.697 N1···N2 2.609	N1···N2 2.710	N1···N2 2.691
N–P–N	N1–P1–N2 104.26(6)	N1–P1–N2 106.08(6)	N2–P1–N1 106.00(18)	N2–P1–N1 108.42(18)	N1–P1–N2 115.72(9) N3–P2–N4 108.86(9)	N1–P1–N2 117.15(7)	N1–P1–N2 116.33(8)
C–P–C	C7–P1–C1 100.05(6)	C7–P1–C1 101.25(7)	C7–P1–C1 101.91(19)	C7–P1–C1 100.28(17)	C1–P1–C7 102.28(9) C35–P2–C41 103.55(9)	C7–P1–C1 101.04(7)	C7–P1–C1 101.42(8)
N–M–N	N2–Li1–N1 74.88(10)	N2–Na1–N1 63.61(4)	N2–Na1–N1 64.66(12)	N1–Na1–N2 64.84(12)	N(2′)1–Na1–N1 140.03(7) N3–Na2–N(4′)2 150.75(7)	N(2′)1-K1–N1 115.43(4)	N1–K1–N(2′)1 110.19(5)
M···M	–	Na1···Na1′ 4.307	Na1···Na1′ 4.061(4)	–	Na1···Na1′ 3.894 Na2···Na2′ 3.238	–	–

longer than those of molecules of **9** owing to the higher coordination sphere of the Li ion in **10**.

Two similar crystal structures of [(^{Dip}LNa)$_2$] **11** (**11**·4C_6H_6, and **11**) were obtained (Figure 5) and both contain half a dimeric molecule in the asymmetric unit. The Na ions are *N*,*N′*-chelated in a slightly asymmetric fashion [the Na–N bond lengths differ by ca. 0.16 Å (mean) in each molecule] and the molecule dimerizes by means of an approximate Na···η^6-Dip–arene interaction,[18] with a mean Na···centroid distance of 2.50 Å, to the second ligand. The geometries in both molecules are essentially identical and only slight differences in the Na···arene coordination have been found, plus a difference in the Na···Na separation by approximately 0.25 Å.

The THF adduct [^{Dip}LNa(THF)$_2$] **13** (Figure 6) shows the same overall molecular structure to [^{Dip}LLi(THF)$_2$] **10** with an *N*,*N′*-chelating diiminophosphinate and parts of the molecule are only poorly ordered.

The molecular structure of the THF adduct [{^{Mes}LNa(THF)}$_2$]·0.5C_6H_6 (**14**·0.5C_6H_6) comprises two in-

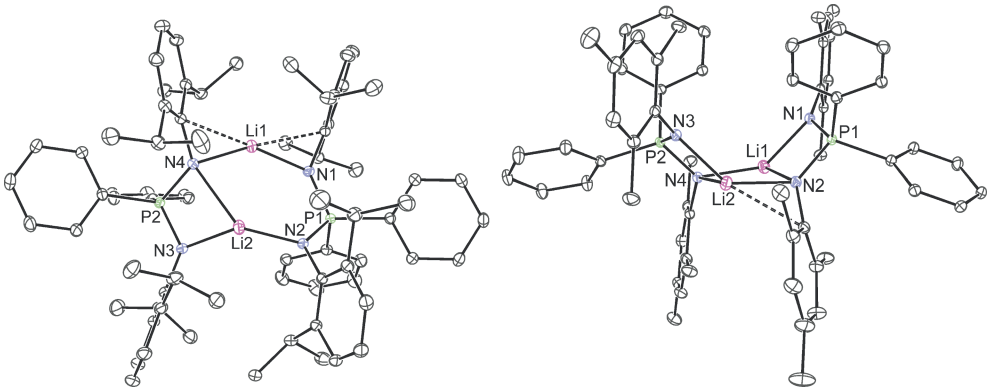

Figure 2. Molecular structure of complexes **5**·C_6H_{14} (left) and **6**·C_6H_6 (right) (30% probability thermal ellipsoids). Only the main Li positions in **5**·C_6H_{14} are shown (65% part). Hydrogen atoms and solvent molecules are omitted for clarity.

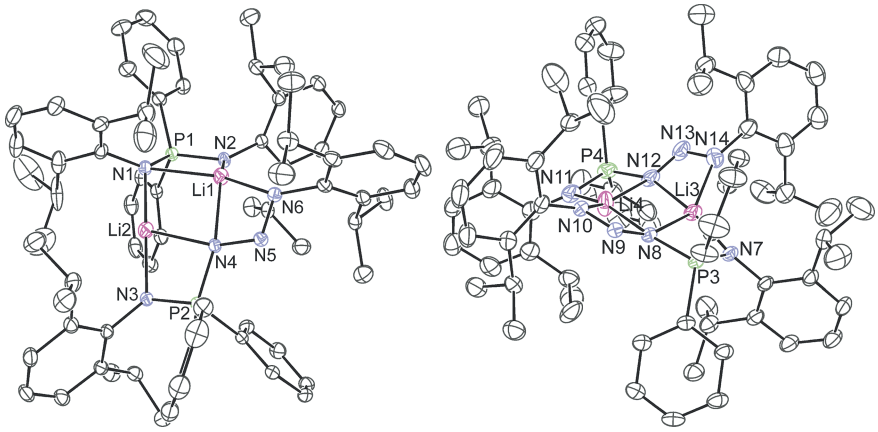

Figure 3. Molecular structure of compound **7**·**8**·C_6H_{14}: **7** (left) and **8** (right) (30% probability thermal ellipsoids). Hydrogen atoms and solvent molecules are omitted for clarity.

dependent half molecules in the asymmetric unit with different Na-diiminophosphinate coordination modes. In **14′** (Figure 7, left), the diiminophosphinate bridges the two Na ions in a 1κ*N*,2κ*N′*-mode, whereas in the other molecule (**14′′**; Figure 7, right) the diiminophosphinate both chelates one Na ion and bridges the second Na centre in a 1κ*N*;1:2κ*N′* mode. In addition, each Na ion in both molecules carries a terminal THF ligand and shows one short contact to one *ortho*-methyl group from a mesityl group. In **14′**, this interaction is formed by means of the mesityl group bound to the nitrogen atom not directly bound to the Na centre in question, and in **14′′**, it is the mesityl group bound to the nitrogen atom with the longer Na···N chelation contact. This coordination could also be regarded

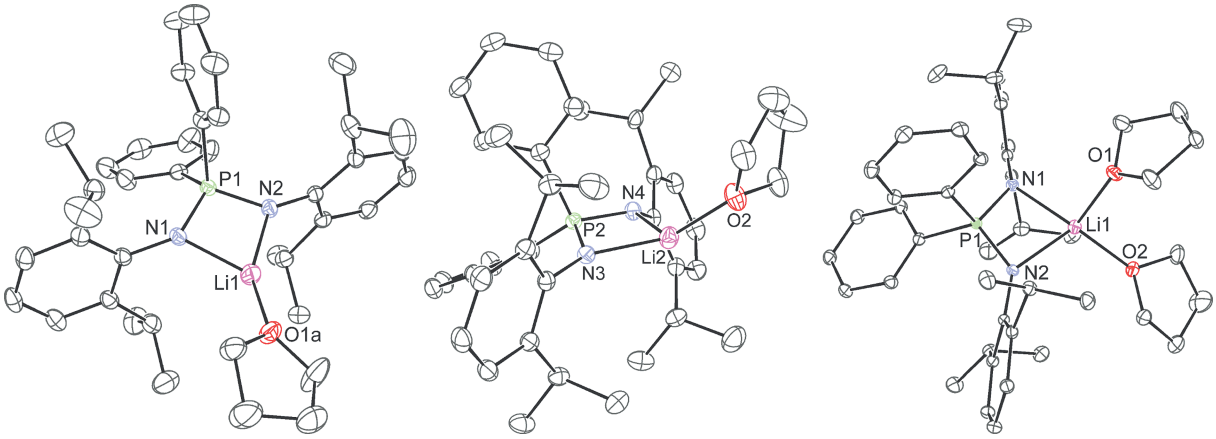

Figure 4. Molecular structure of two independent molecules of **9** (**9′**, left; **9′′**, middle) and **10** (right) (30% probability thermal ellipsoids). Only the main THF contributions are shown for the disordered THF ligands. Hydrogen atoms have been omitted for clarity.

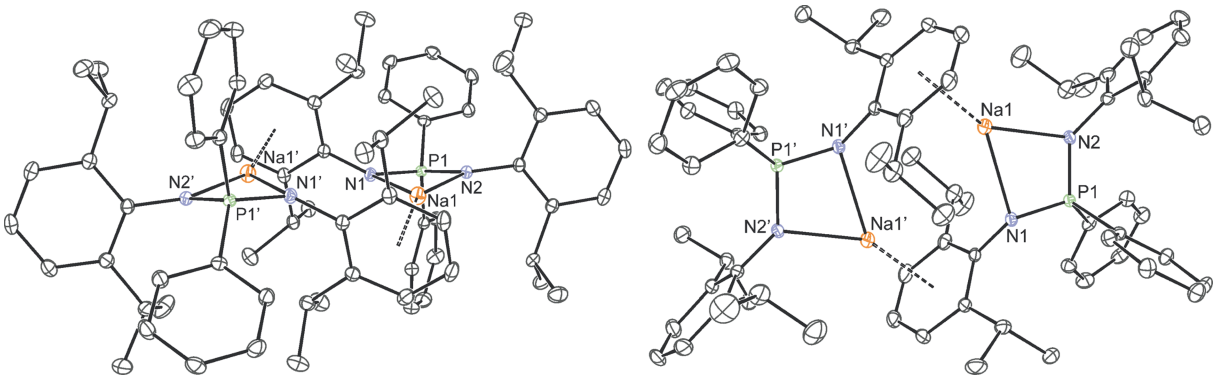

Figure 5. Molecular structure of compound **11**·4C_6H_6 (left) and **11** (right) (30% probability thermal ellipsoids) in two different views. Hydrogen atoms and solvent molecules have been omitted for clarity.

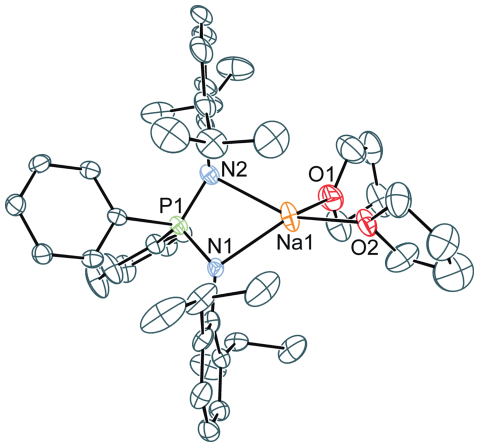

Figure 6. Molecular structure of [^{Dip}LNa(THF)$_2$] **13** (30% probability thermal ellipsoids). Only the main part of the disordered THF molecule on O2 is shown. Hydrogen atoms are omitted for clarity.

as an N,CH_3-chelation in **14′**, and an *N*,*N′*,CH_3-chelation in **14′′**. Several different structure modes for diiminophosphinato alkali metal complexes that bear *N*-bound trimethylsilyl groups and additional THF ligands have previously been described that show a wide variety of geometries. A similar overall structure to that found for **14′′** had been identified for a rubidium complex.[13f]

The crystal structures of two related polymorphs of [^{Mes}LK] **16** have been determined; these show a very similar overall geometry and metrical parameters between them (see Table 2). Polymorphs **16′** and **16′′** (Figure 8) crystallized in the monoclinic and triclinic crystal systems, respectively. Both polymorphs form one-dimensional polymeric chains, mainly through 1κ*N*,2κ*N′* interactions plus various short K···arene interactions[18] in the solid state.

For comparison, the molecular structure of [^{Dip}LK] **15** has previously been described.[7] Complex **15** also forms one-dimensional chains in the solid state as determined for **16**, though the coordination in the former and sterically more demanding complex is exclusively achieved by means of K···arene interactions (see Figure 9) with no K···N contacts.

Across the investigated alkali metal complexes, the diiminophosphinates ^{Dip}L$^-$ and ^{Mes}L$^-$ show a large range of possible N···N separations and are able to accommodate metal ions with a range of ionic radii. The N···N separation ranges from approximately 2.48 Å in the Li complex **9** up to approximately 2.71 Å in the potassium complex **16** and approximately 2.79 Å as previously found for **15**;[7] and they

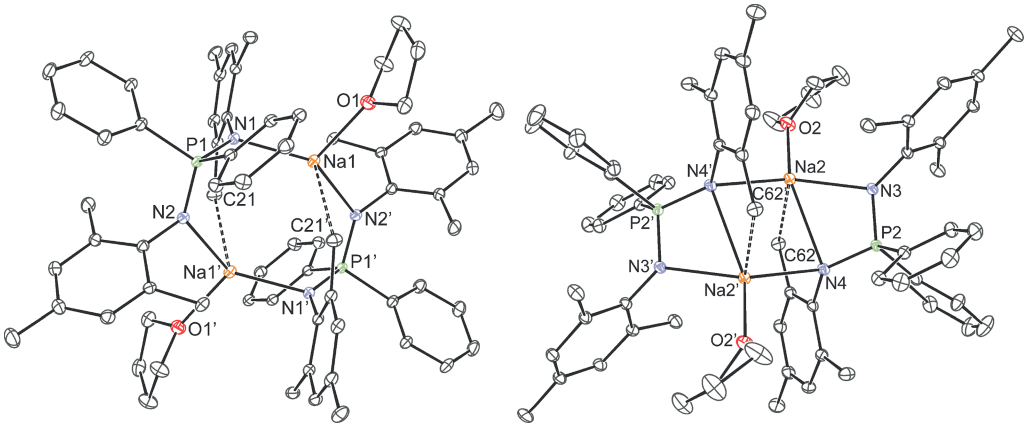

Figure 7. Two independent molecules in the molecular structure of **14**·0.5C_6H_6; molecule **14′** (left) and molecule **14′′** (right) (30% probability thermal ellipsoids). Hydrogen atoms and solvent molecules have been omitted for clarity.

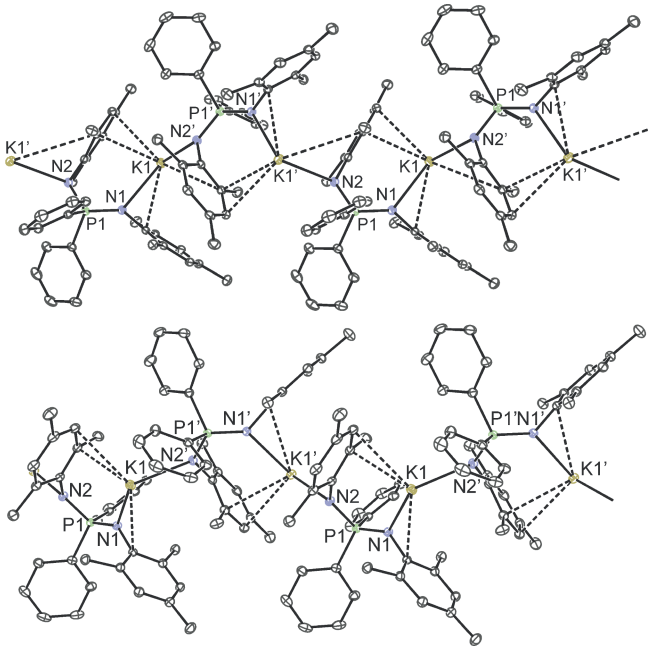

Figure 8. Excerpts of the 1D polymers of two polymorphs of [^{Mes}LK] **16**: **16′** (top) and **16′′** (bottom) (30% probability thermal ellipsoids). Hydrogen atoms have been omitted for clarity.

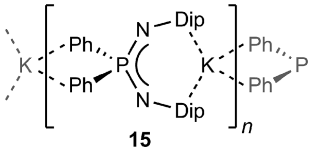

Figure 9. The polymeric chain of [^{Dip}LK] **15**.

can be as short as approximately 2.44 Å as found for ^{Dip}L complexes of divalent Zn.[7] Even shorter respective distances have been found for other diiminophosphinate ligands with small transition-metal ions (approximately down to 2.37–2.38 Å).[19]

Despite their different geometries in the solid state, the solution structures of the alkali metal complexes of ^{Dip}L and ^{Mes}L are highly symmetric on the NMR spectroscopic timescale owing to low energy barriers for these ionic complexes. This is observed for complexes in neat deuterated benzene, with the addition of various amounts of THF or as dissolved THF solvates. As an example, only one doublet and one septet are found for the isopropyl resonances in ^{Dip}L complexes plus the corresponding ^{13}C{^{1}H} NMR spectroscopic resonances, and a comparable number of resonances for the related ^{Mes}L complexes. This is in line with low-temperature studies on the highly soluble heteroleptic [^{Dip}LZnEt] complex,[7] which starts showing resonance splitting only below –70 °C. In contrast, the aminoiminophosphorane Ph$_2$P(=NMes)NHMes **4** shows, like its Dip congener **3**,[7] two sets of resonances for the two different *N*-aryl substituents. Small $^7J_{P,H}$ and $^5J_{P,H}$ couplings were resolved in the ^{1}H NMR spectra for some ^{Mes}L complexes and show a splitting of *para*- and *ortho*-mesityl methyl protons through long-range P–H-couplings with small coupling constants, which disappear in a ^{31}P-decoupled ^{1}H NMR spectrum as found for **12**. The $^7J_{P,H}$ couplings are slightly larger than $^5J_{P,H}$ ones and comparable to those previously found for some aromatic phosphorus compounds.[20] The lithium complexes [(^{Dip}LLi)$_2$] **5**, [(^{Mes}LLi)$_2$] **6** and [^{Dip}LLi(THF)] **9** show a singlet in their respective ^{31}P{^{1}H} NMR spectra at around δ = –3 to –8 ppm, and a singlet or dominating singlet in their ^{7}Li NMR spectra. Dissolved isolated crystals of [^{Dip}LLi(THF)$_2$] **10** in deuterated benzene, however, show somewhat resolved ^{31}P–^{7}Li coupling at room temperature with a broadened doublet (J = 7.2 Hz) in its ^{7}Li NMR spectrum and an unresolved multiplet in its ^{31}P{^{1}H} NMR spectrum.

Conclusion

We have presented the synthesis of the new aminophosphine Ph$_2$PNHMes **2**, aminoiminophosphorane ^{Mes}LH **4** and a series of Li, Na and K complexes of the diiminophosphinates ^{Dip}L$^-$ and ^{Mes}L$^-$. Structural studies show that *N*,*N′*-chelation is the dominant structural feature, but various bridging coordination modes and additional interactions have been observed and include C–H···M and arene···M contacts; these resulted in a variety of different overall structures and some polymorphism. Ligands ^{Dip}L$^-$ and ^{Mes}L show a wide range of N···N separations in the characterized complexes that help accommodate metal ions of various sizes. This study provides further evidence that the tetrahedral P^V centres behave in a more flexible manner than related CN-based ligand backbones. The structural diversity in the characterized complexes and their symmetric solution behaviour suggests that very small energetic changes are required for their interconversion, and some of the crystal structures can be considered snapshots of solution behaviour.

Experimental Section

General Considerations: All manipulations were carried out using standard Schlenk and glovebox techniques under an atmosphere of high-purity dinitrogen. Benzene, toluene, tetrahydrofuran and hexane were dried and distilled from molten potassium, and Et$_2$O was dried and distilled from Na/K alloy. ^{1}H, ^{7}Li, ^{7}Li{^{1}H}, ^{13}C{^{1}H} and ^{31}P{^{1}H} NMR spectra were recorded with a Bruker DPX 300 or Bruker Avance 400 spectrometer in deuterated benzene and were referenced to the residual ^{1}H or ^{13}C{^{1}H} resonances of the solvent used, or external aqueous LiCl or H$_3$PO$_4$ solutions, respectively. IR spectra were recorded with a Perkin–Elmer RXI FTIR spectrometer as Nujol mulls between NaCl plates or on neat solids (or protected with a thin layer of nujol) with an Agilent Cary 630 ATR FTIR spectrometer. Melting points were determined in sealed glass capillaries under dinitrogen and are uncorrected. Elemental analyses were performed by the Elemental Analysis Service at London Metropolitan University or by the Microanalytical Laboratory at the Department of Chemistry, University of Otago. The compounds Ph$_2$P(=NDip)NHDip, ^{Dip}LH **3**[7] and MesN$_3$[21] were reported previously. All other reagents were used as received from commercial sources.

$Ph_2PNHMes$ (2): *n*-Butyllithium (43.0 mL of a 1.62 M solution in hexanes, 69.7 mmol) was slowly added to a solution of freshly distilled $MesNH_2$ (10.0 mL, 9.62 g, 69.1 mmol) in diethyl ether (60 mL) at –80 °C. The mixture was stirred for one hour with slow warming to room temperature. The resulting white suspension was cooled to –80 °C and a solution of Ph_2PCl (12.0 mL, 14.7 g, 67.1 mmol) in Et_2O (60 mL) was slowly added, then the mixture was stirred overnight with slow warming to room temperature. The mixture was filtered, the residue extracted again with diethyl ether (50 mL), then the combined solution was concentrated under reduced pressure to approximately 90 mL and cooled to –30 °C to afford a first crop of crystalline $MesNHPPh_2$ **2**. Concentration of the supernatant solution to approximately 40 mL and cooling to –30 °C afforded a second crop of crystals. A third crop was obtained after further concentration (to ca. 25 mL) and cooling. The isolated solids were dried under vacuum, yield 15.0 g (70%); m.p. 96–100 °C (melts), decomposes at approximately 300 °C. $C_{21}H_{22}NP$ (319.39): calcd. C 78.97, H 6.94, N 4.39; found C 78.47, H 6.80, N 4.22. ^{1}H NMR (C_6D_6, 300.1 MHz, 303 K): δ = 2.09 (s, 6 H, *o*-CH_3), 2.14 (s, 3 H, *p*-CH_3), 3.55 (d, $J_{P,H}$ = 8.4 Hz, 1 H, N*H*), 6.74 (s, 2 H, *m*-Ar*H*), 7.03–7.17 (m, 6 H, Ar*H*), 7.42–7.53 ppm (m, 4 H, Ar*H*). ^{13}C{^{1}H} NMR (C_6D_6, 100.6 MHz, 300 K): δ = 19.1 (d, $J_{P,C}$ = 6.1 Hz, *o*-CH_3), 20.6 (*p*-CH_3), 128.6 (d, $J_{P,C}$ = 6.3 Hz, Ar–C), 128.8 (Ar–C), 129.7 (d, $J_{P,C}$ = 1.2 Hz, Ar*C*), 130.8 (d, $J_{P,C}$ = 3.5 Hz, Ar–C), 131.5 (Ar–C), 131.7 (Ar–C), 140.7 (d, $J_{P,C}$ = 14.2 Hz, Ar–C), 143.1 ppm (d, $J_{P,C}$ = 15.7 Hz, Ar–C). ^{31}P{^{1}H} NMR (C_6D_6, 121.5 MHz, 303 K): δ = 34.7 (s) ppm. IR (solid, ATR): $\tilde{\nu}$ = 3271 (br. m, NH) , 2910 (m), 2853 (m), 1478 (s), 1430 (s), 1363 (m), 1304 (w), 1245 (m), 1218 (s), 1156 (m), 1090 (m), 1066 (m), 1026 (m), 873 (m), 851 (s), 737 (s), 714 (m), 692 (s) cm^{-1}.

$Ph_2P(=NMes)(NHMes)$ [^{Mes}LH (4)]: A slurry of $Ph_2PNHMes$ **2** (8.07 g, 25.3 mmol, 1.0 equiv.) in toluene (20 mL) was transferred with a wide cannula to a solution of cooled (–80 °C) mesitylazide (ca. 5.36 g, 33.3 mmol, 1.3 equiv.) in toluene (30 mL). The mixture was stirred overnight while slowly warming to room temperature with evolution of nitrogen gas. The mixture was stirred for one hour at 60 °C, after which all volatiles were removed under reduced pressure. The solid was recrystallized from hot (ca. 60 °C) *n*-hexane (ca. 100 mL) to yield a white crystalline solid, ^{Mes}LH **4**. The supernatant solution was concentrated to approximately 50 mL and cooled to 4 °C to afford a second crop of crystals. Further filtration, concentration and cooling to 4 °C yielded a third crop. The combined solid was dried under vacuum, yield 12.4 g (92%); m.p. 194–195 °C (melts). $C_{30}H_{33}N_2P$ (452.58): calcd. C 79.62, H 7.35, N 6.19; found C 78.95, H 7.24, N 5.99. ^{1}H NMR (C_6D_6, 400.2 MHz, 300 K): δ = 2.04 (s, 3 H, CH_3), 2.11 (s, 12 H, CH_3), 2.24 (s, 3 H, CH_3), 3.97 (br. d, $J_{P,H}$ ≈ 4 Hz, 1 H, N*H*), 6.62 (s, 2 H, *m*-Ar*H*), 6.89 (s, 2 H, *m*-Ar*H*), 6.95–7.06 (m, 6 H, Ar*H*), 7.74–7.82 (m, 4 H, Ar*H*) ppm. ^{13}C{^{1}H} NMR (C_6D_6, 75.5 MHz, 303 K): δ = 20.6 (CH_3), 20.8 (CH_3), 21.0 (CH_3), 21.3 (CH_3), 127.1 (br., Ar*C*), 128.2 (d, $J_{P,C}$ = 12.9 Hz, Ar*C*), 129.1 (Ar*C*), 129.7 (Ar*C*), 131.0 (d, $J_{P,C}$ = 2.8 Hz, Ar*C*), 131.2 (br. d, $J_{P,C}$ ≈ 7.4 Hz, Ar*C*), 132.2 (d, $J_{P,C}$ = 9.5 Hz, Ar*C*), 134.7 (Ar*C*), 135.3 (Ar*C*), 135.8 (Ar*C*), 135.9 (d, $J_{P,C}$ = 126.6 Hz, Ar*C*), 144.5 (Ar*C*) ppm. ^{31}P{^{1}H} NMR (C_6D_6, 121.5 MHz, 303 K): δ = –16.7 (s) ppm. IR (solid, ATR): $\tilde{\nu}$ = 3339 (m, NH) , 2918 (s), 2853 (s), 1478 (s), 1458 (m), 1449 (m), 1435 (s), 1375 (s), 1370 (s), 1340 (m), 1308 (m), 1290 (m), 1214 (s), 1150 (m), 1111 (s), 1057 (m), 1028 (m), 883 (m), 860 (m), 853 (s), 784 (m), 751 (s), 735 (m), 720 (m), 709 (m), 697 (s) cm^{-1}.

Synthesis of [(^{Dip}LLi)$_2$] (5) and [(^{Dip}L)(^{DipN2}L)Li$_2$]·[(^{DipN2}L)$_2$Li$_2$] (7·8): *n*-Butyllithium (0.64 mL of a 1.6 M solution in hexanes, 1.02 mmol) was slowly added to a solution of ^{Dip}LH **3** (0.50 g, 0.932 mmol) in *n*-hexane (6 mL) at –20 °C. The mixture was stirred for 30 min at room temperature and concentrated to approximately 3 mL to afford colourless crystalline [(^{Dip}LLi)$_2$] **5**. Storage of the supernatant solution at 4 °C afforded a second crop. The isolated material was dried under vacuum. Crystals of [(^{Dip}LLi)$_2$]·C_6H_{14}, **5**·C_6H_{14}, were obtained from a concentrated solution in *n*-hexane at room temperature. A small crop of crystals of [(^{Dip}L)(^{DipN2}L)-Li$_2$]·[(^{DipN2}L)$_2$Li$_2$]·C_6H_{14}, **7·8**·C_6H_{14}, was obtained from *n*-hexane at 4 °C, from a late crop using ^{Dip}LH **3** with some contamination of ^{DipN2}LH present.

Data for [(^{Dip}LLi)$_2$] (5): Yield 0.31 g (61%); it became slowly softer above approximately 110 °C, slowly turning light brown above 130 °C, and brown at approximately 250 °C. ^{1}H NMR (C_6D_6, 300.1 MHz, 303 K): δ = 0.96 [d, *J* = 6.8 Hz, 48 H, CH(C*H*$_3$)$_2$], 3.58 [sept, *J* = 6.8 Hz, 8 H, C*H*(CH_3)$_2$], 6.77–7.42 (m, 32 H, Ar–H) ppm. ^{7}Li NMR (C_6D_6, 155.5 MHz, 300 K): δ = –0.8 ppm (s). ^{13}C{^{1}H} NMR (C_6D_6, 75.5 MHz, 303 K): δ = 24.7 [CH(*C*H$_3$)$_2$], 29.1 [*C*H(CH_3)$_2$], 121.5 (d, $J_{P,C}$ = 3.0 Hz, Ar–*C*), 124.0 (d, $J_{P,C}$ = 2.2 Hz, Ar–*C*), 127.8 (d, $J_{P,C}$ = 11.0 Hz, Ar–*C*), 129.9 (d, $J_{P,C}$ = 2.6 Hz, Ar–*C*), 132.0 (d, $J_{P,C}$ = 8.0 Hz, Ar–*C*), 140.3 (d, $J_{P,C}$ = 94.3 Hz, Ar–*C*), 145.0 (d, $J_{P,C}$ = 6.0 Hz, Ar–*C*), 145.6 (Ar–*C*) ppm. ^{31}P{^{1}H} NMR (C_6D_6, 121.5 MHz, 303 K): δ = –6.7 (s) ppm. IR (nujol): $\tilde{\nu}$ = 1588 (w), 1460 (s), 1435 (s), 1377 (s), 1360 (m), 1350 (m), 1331 (m), 1256 (m), 1191 (m), 1113 (s), 1046 (m), 1010 (m), 789 (m), 780 (m), 750 (m), 722 (m), 710 (m), 696 (s) cm^{-1}.

Data for [(^{Dip}L)(^{DipN2}L)Li$_2$]·[(^{DipN2}L)$_2$Li$_2$] (7·8): ^{1}H NMR (C_6D_6, 300.1 MHz, 303 K): δ = 0.50 [d, *J* = 6.8 Hz, 6 H, CH(C*H*$_3$)$_2$], 0.76–1.38 [m of overlapping d, 90 H, CH(C*H*$_3$)$_2$; overlapping sharp d from 0.85–1.05; overlapping br. d from 1.06–1.38], 2.95 [sept, *J* = 6.8 Hz, 2 H, C*H*(CH_3)$_2$], 3.16 [sept, *J* = 6.8 Hz, 2 H, C*H*(CH_3)$_2$], 3.38–3.84 [m of overlapping sept, *J* = 6.8 Hz, 12 H, C*H*(CH_3)$_2$; overlapping sharp sept from 3.38–3.62; overlapping br. sept from 3.56–3.84], 6.91–7.20 (m, 48 H, Ar–H), 7.50–7.70 (m, 16 H, Ar–H) ppm. ^{31}P{^{1}H} NMR (C_6D_6, 121.5 MHz, 303 K): δ = 4.1, 19.4, 24.0 (3s) ppm. IR (nujol): $\tilde{\nu}$ = 1588 (w), 1464 (s), 1435 (s), 1377 (s), 1360 (m), 1331 (m), 1254 (m), 1199 (m), 1115 (s), 1098 (m), 1049 (m), 1012 (m), 997 (m), 778 (m), 764 (m), 758 (m), 745 (m), 720 (m), 710 (m), 694 (s) cm^{-1}.

[(^{Mes}LLi)$_2$] (6): A solution of *n*-butyllithium (2.0 mL of a 1.6 M solution in hexanes, 1.11 equiv.) was added to a cooled (–70 °C) solution ^{Mes}LH **4** (1.31 g, 2.89 mmol, 1.0 equiv.) in toluene (30 mL) and stirred overnight whilst allowing slow warming to room temperature. The mixture was filtered, and the residual solid was dried under vacuum. The supernatant solution was concentrated to 20 mL under reduced pressure before being cooled to –30 °C to yield a second crop of crystalline solid. Further concentration to approximately 8 mL and cooling afforded a third crop. Isolated crops were dried under vacuum (yield 75%). Crystals of [(^{Mes}LLi)$_2$]·C_6H_6 (**6**·C_6H_6) were obtained by cooling a saturated solution in benzene from 60 °C to room temperature. The ^{13}C{^{1}H} NMR spectroscopic data is given at 60 °C owing to the improved solubility. The ^{1}H NMR spectra at room temperature and 60 °C are essentially identical, yield 1.00 g (75%); m.p. 130–132 °C (melts), decomp. > 310°. $C_{60}H_{64}Li_2N_4P_2$ (917.02): calcd. C 78.59, H 7.03, N 6.11; found C 78.04, H 6.93, N 5.88. ^{1}H NMR (C_6D_6, 300.1 MHz, 303 K): δ = 2.07 (s, 24 H, *o*-CH_3), 2.17 (d, $J_{P,H}$ = 2.1 Hz, 12 H, *p*-CH_3), 6.85 (s, 8 H, *m*-Ar*H*), 6.85–7.15 (m, 12 H, Ar*H*), 7.60–7.69 ppm (m, 8 H, Ar*H*). ^{7}Li{^{1}H} NMR (C_6D_6, 155.5 MHz, 300 K): δ = 2.9 (s and m) ppm. ^{13}C{^{1}H} NMR (C_6D_6, 75.5 MHz, 333 K): δ = 20.7 (d, $J_{P,C}$ = 0.8 Hz, CH_3), 21.5 (CH_3), 127.8 (Ar*C*, partially hidden by solvent resonance), 130.2 (d, $J_{P,C}$ = 1.8 Hz, Ar*C*), 131.5 (d, $J_{P,C}$ = 8.6 Hz, Ar*C*), 134.2 (d, $J_{P,C}$ = 6.0 Hz, Ar*C*), 139.9 (br. d, $J_{P,C}$ = 95.5 Hz, Ar*C*), 144.5 (br., Ar*C*) ppm. Two

$^{13}C\{^1H\}$ NMR spectroscopic resonances are missing despite a long acquisition time and are either hidden underneath the strong solvent signal or broadened into the baseline. $^{31}P\{^1H\}$ NMR (C_6D_6, 121.5 MHz, 303 K): δ = –3.0 (s) ppm. IR (solid, ATR): $\tilde{\nu}$ = 2919 (s), 2852 (s), 1474 (s), 1458 (m), 1448 (m), 1435 (s), 1370 (s), 1329 (m), 1306 (m), 1285 (m), 1214 (s), 1151 (m), 1111 (s), 1058 (m), 1021 (m), 997 (m), 880 (m), 859 (m), 853 (s), 751 (m), 735 (m), 720 (m), 697 (s) cm^{-1}.

Synthesis of [^{Dip}LLi(THF)] (9) and [^{Dip}LLi(THF)$_2$] (10): Crops of crystalline **9** and **10** were obtained by recrystallizing small quantities of [(^{Dip}LLi)$_2$] **5** from *n*-hexane either with a few drops of THF (**9**) or from an *n*-hexane/THF (ca. 8:1) mixture (**10**) at 4 °C. NMR spectra of isolated colourless crystals of **9** and **10** are very similar except for different THF-proton integration and $^7Li/^{31}P$ NMR spectroscopic multiplicities.

Data for [^{Dip}LLi(THF)] (9): ^1H NMR (C_6D_6, 400.2 MHz, 294 K): δ = 1.03 (m_c, 4 H, THF–CH_2), 1.06 [d, J = 6.8 Hz, 24 H, CH(CH_3)$_2$], 3.24 (m_c, 4 H, THF–OCH_2), 3.84 [sept, J = 6.8 Hz, 4 H, CH(CH_3)$_2$], 6.91–7.23 (m, 12 H, Ar–H), 7.51–7.57 (m, 4 H, Ar–H) ppm. ^7Li NMR (C_6D_6, 155.5 MHz, 294 K): δ = 1.78 ppm (s, sharp). $^{13}C\{^1H\}$ NMR (C_6D_6, 100.6 MHz, 295 K): δ = 24.1 [CH(CH$_3$)$_2$], 25.2 (THF–CH$_2$), 29.1 [CH(CH_3)$_2$], 68.8 (THF–OCH$_2$), 120.7 (d, $J_{P,C}$ = 3.1 Hz, Ar–C), 123.5 (d, $J_{P,C}$ = 2.0 Hz, Ar–C), 127.5 (d, $J_{P,C}$ = 11.0 Hz, Ar–C), 129.5 (d, $J_{P,C}$ = 2.6 Hz, Ar–C), 131.7 (d, $J_{P,C}$ = 8.0 Hz, Ar–C), 140.0 (d, $J_{P,C}$ = 93.4 Hz, Ar–C), 144.4 (d, $J_{P,C}$ = 6.0 Hz, Ar–C), 146.3 (Ar–C) ppm. $^{31}P\{^1H\}$ NMR (C_6D_6, 121.5 MHz, 303 K): δ = –7.7 (s) ppm. IR (nujol): $\tilde{\nu}$ = 1588 (w), 1461 (s), 1430 (s), 1378 (m), 1366 (s), 1321 (m), 1269 (s), 1230 (m), 1216 (m), 1111 (m), 1100 (m), 1050 (m), 1015 (m), 794 (m), 775 (m), 753 (m), 710 (m), 698 (s) cm^{-1}.

Data for [^{Dip}LLi(THF)$_2$] (10): ^1H NMR (C_6D_6, 300.1 MHz, 303 K): δ = 1.06 [d, J = 6.8 Hz, 24 H, CH(CH_3)$_2$], 1.27 (m_c, 8 H, THF–CH_2), 3.44 (m_c, 8 H, THF–OCH_2), 3.84 [sept, J = 6.8 Hz, 4 H, CH(CH_3)$_2$], 6.92–7.26 (m, 12 H, Ar–H), 7.50–7.62 (m, 4 H, Ar–H) ppm. ^7Li NMR (C_6D_6, 155.5 MHz, 300 K): δ = 1.72 ppm (br. d, $J_{P,Li}$ = 7.2 Hz). $^{13}C\{^1H\}$ NMR (C_6D_6, 75.5 MHz, 303 K): δ = 24.2 [CH(CH$_3$)$_2$], 25.5 (THF-CH$_2$), 29.0 [CH(CH_3)$_2$], 68.4 (THF–OCH$_2$), 120.7 (d, $J_{P,C}$ = 2.9 Hz, Ar–C), 123.5 (d, $J_{P,C}$ = 2.1 Hz, Ar–C), 127.5 (d, $J_{P,C}$ = 10.9 Hz, Ar–C), 129.4 (d, $J_{P,C}$ = 2.6 Hz, Ar–C), 131.7 (d, $J_{P,C}$ = 8.1 Hz, Ar–C), 140.1 (d, $J_{P,C}$ = 93.5 Hz, Ar–C), 144.3 (d, $J_{P,C}$ = 6.0 Hz, Ar–C), 146.5 (Ar–C) ppm. $^{31}P\{^1H\}$ NMR (C_6D_6, 121.5 MHz, 303 K): δ = –7.8 (m) ppm. IR (nujol): $\tilde{\nu}$ = 1585 (w), 1462 (s), 1431 (s), 1377 (s), 1355 (m), 1324 (s), 1275 (s), 1215 (m), 1104 (s), 1072 (m), 1052 (s), 1017 (m), 993 (m), 903 (m), 765 (s), 750 (m), 710 (m), 699 (s) cm^{-1}.

[(^{Dip}LNa)$_2$] (11): Toluene (20 mL) was added to a mixture of ^{Dip}LH **3** (1.02 g, 1.90 mmol, 1.0 equiv.) and [Na{N(SiMe$_3$)$_2$}] (0.37 g, 2.00 mmol, 1.05 equiv.) at 0 °C and vigorously stirred overnight with slow warming to room temperature. The formed precipitate of **11** was removed by filtration, washed with *n*-hexane (10 mL) and dried under vacuum. The supernatant solution was concentrated to approximately 8 mL under reduced pressure and cooled to 4 °C to afford a second crop of **11** in 72% yield. Crystals of [(^{Dip}LNa)$_2$] **11** were obtained from a toluene/*n*-hexane mixture and crystals of [(^{Dip}LNa)$_2$]·4C_6H_6 (**11**·4C_6H_6) were obtained from warm benzene, yield 0.77 g (72%); m.p. 170–172 °C (melts), 247–250 °C (decomp). The NMR spectra were recorded and are given at elevated temperatures owing to the poor solubility in aromatic solvents at room temperature. No significant differences between spectra recorded at 25 or 65 °C were found. ^1H NMR (C_6D_6, 300.1 MHz, 338 K): δ = 0.98 [d, J = 6.9 Hz, 48 H, CH(CH_3)$_2$], 3.71 [sept, J = 6.9 Hz, 8 H, CH(CH_3)$_2$], 6.93–7.05 (m, 16 H, Ar–H), 7.10–7.16 (m, 8 H, Ar–H), 7.37–7.48 (m, 8 H, Ar–H) ppm. $^{13}C\{^1H\}$ NMR (C_6D_6, 75.5 MHz, 338 K): δ = 24.2 [CH(CH$_3$)], 28.5 [CH(CH_3)], 120.0 (d, $J_{P,C}$ = 2.9 Hz, ArC), 123.6 (d, $J_{P,C}$ = 2.0 Hz, ArC), 127.4 (d, $J_{P,C}$ = 10.9 Hz, ArC), 129.0 (d, $J_{P,C}$ = 2.6 Hz, ArC), 131.5 (d, $J_{P,C}$ = 7.9 Hz, ArC), 141.3 (d, $J_{P,C}$ = 97.6 Hz, ArC), 144.4 (d, $J_{P,C}$ = 6.0 Hz, ArC), 147.3 (d, coupling not resolved, ArC) ppm. $^{31}P\{^1H\}$ NMR (C_6D_6, 121.5 MHz, 298 K): δ = –14.6 (s) ppm. $^{31}P\{^1H\}$ NMR (C_6D_6, 121.5 MHz, 338 K): δ = –14.2 (s) ppm. IR (nujol): $\tilde{\nu}$ = 1586 (w), 1461 (s), 1377 (s), 1367 (s), 1327 (m), 1324 (s), 1273 (m), 1215 (m), 1112 (m), 1097 (m), 1050 (m), 1014 (m), 989 (m), 933 (m), 775 (m), 744 (m), 699 (m) cm^{-1}.

[^{Mes}LNa] (12) and [{^{Mes}LNa(THF)}$_2$] (14): Toluene (30 mL) was added to a mixture of ^{Mes}LH **4** (0.97 g, 2.14 mmol, 1.0 equiv.) and [Na{N(SiMe$_3$)$_2$}] (0.45 g, 2.46 mmol, 1.15 equiv.) at 0 °C and vigorously stirred overnight with gradual warming to room temperature. The formed precipitate was removed by filtration, washed with *n*-hexane (15 mL) and dried under vacuum to afford **12** of a yet undetermined structure (yield 71%). Compound **12** was only poorly soluble in noncoordinating solvents and thus a few drops of THF were added to acquire solution NMR spectroscopic data, yield 0.72 g (71%); m.p. 313–317 °C (melts). $C_{30}H_{32}N_2NaP$ (474.56): calcd. C 75.93, H 6.80, N 5.90; found C 75.78, H 6.68, N 5.79. ^1H NMR [C_6D_6/THF (ca. 30:1, THF resonances are not given), 300.1 MHz, 298 K]: δ = 2.24 (d, $J_{P,H}$ = 1.8 Hz, 24 H, *o*-CH_3), 2.29 (d, $J_{P,H}$ = 0.9 Hz, 12 H, *p*-CH_3), 6.88 (s, 8 H, *m*-ArH), 7.02–7.16 (m, 12 H, ArH), 7.80–7.89 (m, 8 H, ArH) ppm. $^{13}C\{^1H\}$ NMR [C_6D_6/THF (ca. 30:1, THF resonances are not given), 75.5 MHz, 298 K]: δ = 20.9 (d, $J_{P,C}$ = 1.2 Hz, CH_3), 21.8 (d, $J_{P,C}$ = 0.9 Hz, CH_3), 126.3 (vbr., ArC), 127.3 (d, $J_{P,C}$ = 11.0 Hz, ArC), 128.8 (br., ArC), 129.3 (d, $J_{P,C}$ = 2.3 Hz, ArC), 131.6 (d, $J_{P,C}$ = 8.3 Hz, ArC), 132.9 (br. d, $J_{P,C}$ = 6.6 Hz, ArC), 141.6 (d, vbr., $J_{P,C}$ ≈ 94 Hz, ArC), 148.0 (vbr., ArC) ppm. $^{31}P\{^1H\}$ NMR [C_6D_6/THF (ca. 30:1), 121.5 MHz, 298 K]: δ = –14.6 (s) ppm. IR (solid, ATR): $\tilde{\nu}$ = 2920 (m), 2853 (s), 1588 (w), 1472 (s), 1433 (m), 1418 (m), 1375 (m), 1303 (s), 1247 (s), 1215 (m), 1164 (m), 1103 (s), 1029 (s), 979 (m), 942 (m), 851 (s), 821 (w), 763 (m), 749 (m), 698 (s), 658 (m) cm^{-1}.

Crystals of [{^{Mes}LNa(THF)}$_2$]·0.5C_6H_6 (**14**·0.5C_6H_6) were obtained by recrystallizing a small quantity of **12** from toluene/THF (ca. 8:1) at –25 °C. This likely reflects more closely the composition studied by the solution NMR spectroscopic experiments in deuterated benzene/THF.

[^{Mes}LK] (16): Toluene (30 mL) was added to a mixture of ^{Mes}LH **4** (0.54 g, 1.10 mmol, 1.0 equiv.) and [K{N(SiMe$_3$)$_2$}] (0.26 g, 1.30 mmol, 1.18 equiv.) at 0 °C and vigorously stirred overnight with slow warming to room temperature. The precipitate was removed by filtration, washed with *n*-hexane (10 mL) and dried under vacuum. A small second crop was isolated after concentration of the supernatant solution and cooling to 4 °C, yield 0.38 g (70%); m.p. 178–180 °C (melts), 216–218 °C (decomp.). $C_{30}H_{32}KN_2P$ (490.67): calcd. C 73.44, H 6.57, N 5.71; found C 73.36, H 6.46, N 5.81. The compound was only poorly soluble in hydrocarbon solvents and the ^1H NMR spectrum was recorded at elevated temperatures. Alternatively, the addition of small quantities of coordinating solvents such as THF enhanced the solubility significantly. ^1H NMR (C_6D_6, 300.1 MHz, 333 K): δ = 2.14 (s, 6 H, *p*-CH_3), 2.24 (s, 12 H, *o*-CH_3), 6.72 (s, 4 H, *m*-ArH), 6.99–7.15 (m, 4 H, Ar–H), 8.02–8.18 (br. m, 6 H, Ar–H) ppm. ^1H NMR [C_6D_6/THF (ca. 5:1, THF resonances not given), 300.1 MHz, 298 K]: δ = 2.16 (s, 6 H, *p*-CH_3), 2.40 (s, 12 H, *o*-CH_3), 6.78 (s, 4 H, *m*-ArH), 7.02–7.17 (m, 4 H, Ar–H), 8.21–8.34 (br. m, 6 H, Ar–H) ppm. $^{13}C\{^1H\}$ NMR [C_6D_6/THF (ca. 5:1, THF resonances not given), 75.5 MHz,

Table 2. Crystallographic data.

	2	**4** (**4′**)	**4** (**4′′**)	**5**·C_6H_{14}	**6**·C_6H_6	**7**·**8**·C_6H_{14}	**9**
Chemical formula	$C_{21}H_{22}NP$	$C_{30}H_{33}N_2P$	$C_{30}H_{33}N_2P$	$C_{78}H_{102}Li_2N_4P_2$	$C_{66}H_{70}Li_2N_4P_2$	$C_{150}H_{190}Li_4N_{14}P_4$	$C_{40}H_{52}LiN_2OP$
Formula mass	319.37	452.55	452.55	1171.46	995.08	2340.80	614.75
Crystal system	monoclinic	monoclinic	triclinic	triclinic	triclinic	monoclinic	triclinic
a [Å]	15.3831(17)	12.0581(4)	11.200(2)	12.295(3)	11.770(2)	25.9411(6)	15.424(3)
b [Å]	4.6094(4)	15.5786(6)	11.300(2)	12.854(3)	13.440(3)	23.3546(6)	15.518(3)
c [Å]	25.954(2)	13.3339(4)	11.660(2)	23.374(5)	17.440(4)	23.5675(6)	16.428(3)
α [°]	90.00	90.00	117.51(3)	89.36(3)	82.36(3)	90.00	105.28(3)
β [°]	106.986(9)	91.628(3)	97.15(3)	82.22(3)	88.38(3)	103.907(3)	95.67(3)
γ [°]	90.00	90.00	101.01(3)	69.34(3)	84.59(3)	90.00	102.52(3)
Unit-cell volume [Å^3]	1760.0(3)	2503.74(15)	1245.8(4)	3422.0(12)	2721.8(10)	13859.7(6)	3651.7(13)
T [K]	123(2)	123(2)	100(2)	100(2)	100(2)	123(2)	173(2)
Space group	$P2_1/c$	$P2_1/n$	$P\bar{1}$	$P\bar{1}$	$P\bar{1}$	$P2_1/c$	$P\bar{1}$
Z	4	4	2	2	2	4	4
Radiation type	Mo-K_α	Mo-K_α	synchrotron	synchrotron	synchrotron	Mo-K_α	Mo-K_α
μ [mm^{-1}]	0.156	0.130	0.131	0.109	0.125	0.109	0.107
No. of reflections measured	10449	26133	23397	60775	65818	55289	32538
No. of independent reflections	3110	7294	6956	17002	12084	24378	17602
Completeness (to θ) [%]	99.8 (at 25.00°)	99.9 (at 30.00°)	98.2 (at 25.00°)	99.7 (at 25.00°)	99.4 (at 27.22°)	99.8 (at 25.00°)	99.7 (at 28.00°)
R_{int}	0.0663	0.0281	0.0510	0.0851	0.0382	0.0325	0.0274
Final R_1 values [$I>2\sigma(I)$]	0.0553	0.0398	0.0464	0.0535	0.0419	0.0792	0.0484
Final $wR(F^2)$ values [$I>2\sigma(I)$]	0.1360	0.1023	0.1178	0.1327	0.1059	0.2103	0.1148
Final R_1 values (all data)	0.0706	0.0532	0.0507	0.0648	0.0457	0.1161	0.0789
Final $wR(F^2)$ values (all data)	0.1494	0.1122	0.1211	0.1436	0.1087	0.2425	0.1305
GoF on F^2	1.054	1.029	1.045	1.070	1.061	1.035	1.032
Largest diff. peak, hole [e Å^{-3}]	0.596, –0.427	0.411, –0.293	0.369, –0.568	0.943, –0.537	0.256, –0.434	1.210, –0.847	0.265, –0.292

Table 2. (continued)

	10	**11**·4C_6H_6	**11**	**13**	**14**·0.5C_6H_6	**16** (**16′**)	**16** (**16′′**)
Chemical formula	$C_{44}H_{60}LiN_2O_2P$	$C_{96}H_{112}N_4Na_2P_2$	$C_{72}H_{88}N_4Na_2P_2$	$C_{44}H_{60}N_2NaO_2P$	$C_{71}H_{83}N_4Na_2O_2P_2$	$C_{30}H_{32}KN_2P$	$C_{30}H_{32}KN_2P$
Formula mass	686.85	1429.82	1117.38	702.90	1132.33	490.65	490.65
Crystal system	monoclinic	monoclinic	triclinic	monoclinic	triclinic	monoclinic	monoclinic
a [Å]	17.060(3)	11.0370(2)	10.2911(5)	17.749(4)	10.325(2)	14.1174(6)	27.755(6)
b [Å]	11.798(2)	18.8288(4)	10.5892(4)	11.828(2)	14.873(3)	11.8508(5)	11.800(2)
c [Å]	20.701(4)	20.3086(4)	15.3253(7)	20.096(4)	20.320(4)	15.7569(6)	18.924(4)
α [°]	90.00	90.00	88.799(4)	90.00	84.38(3)	90.00	90.00
β [°]	105.32(3)	98.047(2)	81.499(4)	102.80(3)	87.57(3)	102.398(4)	124.47(3)
γ [°]	90.00	90.00	73.415(4)	90.00	83.70(3)	90.00	90.00
Unit-cell volume [Å^3]	4018.5(14)	4178.84(14)	1582.61(12)	4114.1(14)	3085.1(11)	2574.69(18)	5109.9(18)
T [K]	100(2)	123(2)	123(2)	123(2)	100(2)	123(2)	100(2)
Space group	Cc	$P2_1/n$	$P\bar{1}$	Cc	$P\bar{1}$	$P2_1/n$	$C2/c$
Z	4	2	1	4	2	4	8
Radiation type	synchrotron	Mo-K_α	Mo-K_α	Mo-K_α	synchrotron	Mo-K_α	synchrotron
μ [mm^{-1}]	0.106	0.110	0.127	0.114	0.134	0.290	0.292
No. of reflections measured	33442	19402	13624	12962	37119	17747	39912
No. of independent reflections	9809	9091	7621	6087	18092	5609	5640
Completeness (to θ) [%]	99.1 (at 25.00°)	99.7 (at 27.00°)	99.6 (at 28.00°)	99.9 (at 25.00°)	91.9 (at 25.00°)	99.9 (at 27.00°)	99.6 (at 27.13°)
R_{int}	0.0507	0.0232	0.0282	0.0379	0.1096	0.0317	0.0604
Final R_1 values [$I>2\sigma(I)$]	0.0363	0.0426	0.1015	0.0568	0.0765	0.0366	0.0418
Final $wR(F^2)$ values [$I>2\sigma(I)$]	0.0897	0.0957	0.2484	0.1353	0.2016	0.0886	0.1027
Final R_1 values (all data)	0.0377	0.0607	0.1109	0.0707	0.0979	0.0484	0.0474
Final $wR(F^2)$ values (all data)	0.0914	0.1044	0.2529	0.1504	0.2189	0.0954	0.1059
GoF on F^2	1.065	1.033	1.135	1.023	1.016	1.039	1.065
Largest diff. peak, hole [e Å^{-3}]	0.391, –0.251	0.366, –0.361	1.243, –0.414	0.345, –0.282	0.954, –0.626	0.403, –0.253	0.405, –0.497

298 K]: δ = 20.7 (CH_3), 22.1 (CH_3), 127.5 (Ar–C), 127.5 (d, $J_{P,C}$ = 11.5 Hz, Ar*C*), 128.6 (d, $J_{P,C}$ = 11.9 Hz, Ar*C*), 129.3 (Ar–C), 131.9 (d, $J_{P,C}$ = 8.6 Hz, Ar*C*) ppm. Note: Three Ar*C* resonances are missing. Two downfield Ar*C* resonances are believed to be broadened into the baseline (compare with the very broad resonances found for **12**) and one is believed to the hidden by the strong solvent resonance. $^{31}P\{^1H\}$ NMR (C_6D_6, 121.5 MHz, 333 K): δ = –17.5 (s) ppm. IR (solid, ATR): $\tilde{\nu}$ = 2952 (m), 2920 (s), 2853 (s), 1458 (s), 1431 (m), 1421 (m), 1376 (m), 1325 (m), 1304 (m), 1285 (m), 1263 (s), 1164 (m), 1103 (m), 1041 (m), 983 (m), 857 (m), 840 (m), 761 (m), 746 (m), 711 (s), 699 (s) cm^{-1}.

X-ray Crystallography: Suitable crystals were mounted in silicone oil and were either measured with an Oxford Xcalibur Gemini Ul-

tra (**2**, **4′**, **7·8**·C_6H_{14}, **11**·4C_6H_6, **11**, **13** and **16′**) or Nonius Kappa (**9**) diffractometer with Mo-K_α radiation (λ = 0.71073 Å) or at the MX1 or MX2 beamlines (**4′′**, **5**·C_6H_{14}, **6**·C_6H_6, **10**, **14**·0.5C_6H_6 and **16′′**) at the Australian Synchrotron using synchrotron radiation with a wavelength close to Mo-K_α radiation. Data collection at the synchrotron was performed using the Blu-Ice software package[22] and data reduction was performed using XDS.[23] All structures were refined using SHELX.[24] All non-hydrogen atoms were refined anisotropically. Semiempirical (multiscan) absorption corrections were performed on all datasets. A low data completeness of 91.9% (at 25.00° θ; and 77.0% at 33.13° $\theta_{max.}$) in the crystal structure of **14**·0.5C_6H_6 is due to the experimental setup at the synchrotron and only one Φ scan could be collected. In **5**·C_6H_{14}, the two Li atoms are disordered and were modelled and refined with two positions each to 65 and 35% parts. In **7·8**·C_6H_{14}, one isopropyl group of **8** is disordered and was modelled using two positions for each carbon atom (55% part for C103–105 and 45% part for C157–C159) and refined using geometry restraints. The lattice *n*-hexane molecule in the same structure is disordered and was modelled with two positions for each carbon atom (two 50% parts) using geometry restraints. In **9**, two isopropyl groups are disordered and were modelled and refined with two positions for C19–C21 (84 and 16% parts) and C71–C73 (48 and 52% parts) using geometry restraints. Two coordinated THF molecules are disordered and were modelled and refined with two positions for O1 and C37–C40 (37 and 63% parts) and C78–C80 (63 and 37% parts) using geometry restraints. In **13**, one coordinated THF molecule is severely disordered and was modelled with two positions for each atom and refined using geometry restraints. Selected bond lengths and angles of all crystal structures are collected in Table 1 and refinement details are summarized in Table 2.

CCDC-1025687 (**2**), -1025688 (**4′**), -1025689 (**4′′**), -1025690 (**5**·C_6H_{14}), -1025691 (**6**·C_6H_6), -1025692 (**7·8**·C_6H_{14}), -1025693 (**9**), -1025694 (**10**), -1025695 (**11**·4C_6H_6), -1025696 (**11**), -1025697 (**13**), -1025698 (**14**·0.5C_6H_6), -1025699 (**16′**), and -1025700 (**16′′**) contain the supplementary crystallographic data for this paper. These data can be obtained free of charge from The Cambridge Crystallographic Data Centre via www.ccdc.cam.ac.uk/data_request/cif.

Acknowledgments

A. S. is grateful to the Australian Research Council for support and a fellowship. Part of this research was undertaken on the MX1 and MX2 beamlines at the Australian Synchrotron, Victoria, Australia.

[1] L. Bourget-Merle, M. F. Lappert, J. R. Severn, *Chem. Rev.* **2002**, *102*, 3031–3065.
[2] a) F. T. Edelmann, *Adv. Organomet. Chem.* **2008**, *57*, 183–352; b) P. J. Bailey, S. Pace, *Coord. Chem. Rev.* **2001**, *214*, 91–141.
[3] a) A. Raghavan, A. Venugopal, *J. Coord. Chem.* **2014**, *67*, 2530–2549; b) N. J. Hill, I. Vargas-Baca, A. H. Cowley, *Dalton Trans.* **2009**, 240–253.
[4] For reviews on low-oxidation-state complexes with bulky *N,N′*-coordinating ligands, see: a) C. Jones, A. Stasch, *Top. Organomet. Chem.* **2013**, *45*, 73–102; b) Y.-C. Tsai, *Coord. Chem. Rev.* **2012**, *256*, 722–758; c) A. Stasch, C. Jones, *Dalton Trans.* **2011**, *40*, 5659–5672; d) M. Asay, C. Jones, M. Driess, *Chem. Rev.* **2011**, *111*, 354–396; e) C. Jones, *Coord. Chem. Rev.* **2010**, *254*, 1273–1289; f) S. K. Mandal, H. W. Roesky, *Chem. Commun.* **2010**, *46*, 6016–6041; g) S. Schulz, *Chem. Eur. J.* **2010**, *16*, 6416–6428; h) Y. Mizuhata, T. Sasamori, N. Tokitoh, *Chem. Rev.* **2009**, *109*, 3479–3511.
[5] A. Steiner, S. Zacchini, P. I. Richards, *Coord. Chem. Rev.* **2002**, *227*, 193–216.
[6] A. Stasch, *Angew. Chem. Int. Ed.* **2014**, *53*, 10200–10203; *Angew. Chem.* **2014**, *126*, 10364–10367.
[7] A. Stasch, *Chem. Eur. J.* **2012**, *18*, 15105–15112.
[8] a) K. Albahily, V. Fomitcheva, S. Gambarotta, I. Korobkov, M. Murugesu, S. I. Gorelsky, *J. Am. Chem. Soc.* **2011**, *133*, 6380–6387; b) K. Albahily, V. Fomitcheva, Y. Shaikh, E. Sebastiao, S. I. Gorelsky, S. Gambarotta, I. Korobkov, R. Duchateau, *Organometallics* **2011**, *30*, 4201–4210; c) K. Albahily, S. Licciulli, S. Gambarotta, I. Korobkov, R. Chevalier, K. Schuhen, R. Duchateau, *Organometallics* **2011**, *30*, 3346–3352.
[9] a) Y. Yang, K. Lv, L. Wang, Y. Wang, D. Cui, *Chem. Commun.* **2010**, *46*, 6150–6152; b) S. Li, D. Cui, D. Li, Z. Hou, *Organometallics* **2009**, *28*, 4814–4822.
[10] For reviews, see: a) Z. Fei, P. Dyson, *Coord. Chem. Rev.* **2005**, *249*, 2056–2074; b) M. Alajarin, C. Lopez-Leonardo, P. Llamas-Lorente, *Top. Curr. Chem.* **2005**, *250*, 77–106.
[11] A. Stasch, *Angew. Chem. Int. Ed.* **2012**, *51*, 1930–1933; *Angew. Chem.* **2012**, *124*, 1966–1969.
[12] a) Y. G. Gololobov, L. F. Kasukhin, *Tetrahedron* **1992**, *48*, 1353–1406; b) Y. G. Gololobov, I. N. Zhmurova, L. F. Kasukhin, *Tetrahedron* **1981**, *37*, 437–472; c) H. Staudinger, J. Meyer, *Helv. Chim. Acta* **1919**, *2*, 635–646.
[13] a) B. Prashanth, S. Singh, *Dalton Trans.* **2014**, *43*, 16880–16888; b) S. A. Ahmed, M. S. Hill, P. B. Hitchcock, S. M. Mansell, O. St John, *Organometallics* **2007**, *26*, 538–549; c) A. J. Edwards, E. Wenger, *Aust. J. Chem.* **2002**, *55*, 249–252; d) M. Schultz, B. F. Straub, P. Hofmann, *Acta Crystallogr., Sect. C* **2002**, *58*, m256–m257; e) E. Müller, J. Müller, H.-G. Schmidt, M. Noltemeyer, F. T. Edelmann, *Phosphorus Sulfur Silicon Relat. Elem.* **1996**, *1*, 121–126; f) Steiner, D. Stalke, *Inorg. Chem.* **1993**, *32*, 1977–1981; g) A. Recknagel, A. Steiner, M. Noltemeyer, S. Brooker, D. Stalke, F. T. Edelmann, *J. Organomet. Chem.* **1991**, *414*, 327–335.
[14] M. W. P. Bebbington, D. Bourissou, *Coord. Chem. Rev.* **2009**, *253*, 1248–1261.
[15] a) W. Q. Tian, Y. A. Wang, *J. Org. Chem.* **2004**, *69*, 4299–4308; b) J. E. Leffler, R. D. Temple, *J. Am. Chem. Soc.* **1967**, *89*, 5235–5246.
[16] a) A. M. Willcocks, T. P. Robinson, C. Roche, T. Pugh, S. P. Richards, A. J. Kingsley, J. P. Lowe, A. L. Johnson, *Inorg. Chem.* **2012**, *51*, 246–257; b) C. Jones, S. J. Bonyhady, N. Holzmann, G. Frenking, A. Stasch, *Inorg. Chem.* **2011**, *50*, 12315–12325; c) G. Jin, C. Jones, P. C. Junk, K.-A. Lippert, R. P. Rose, A. Stasch, *New J. Chem.* **2009**, *33*, 64–75.
[17] One Li complex with a chelating phosphazide fragment has been reported: M. Nieger, E. Niecke, M. Larbig, private communication to the CCDC, structure code DAGWOZ, CCDC number 841785.
[18] G. W. Gokel, L. J. Barbour, S. L. De Wall, E. S. Meadows, *Coord. Chem. Rev.* **2001**, *222*, 127–154.
[19] As determined by a search of the CCDC database, September 2014.
[20] C. E. Griffin, M. Gordon, *J. Am. Chem. Soc.* **1967**, *89*, 4427–4431.
[21] a) D. G. Brown, N. Sanuantrakun, B. Schulze, U. S. Schubert, C. P. Berlinguette, *J. Am. Chem. Soc.* **2012**, *134*, 12354–12357; b) F. Kloss, U. Köhn, B. O. Jahn, M. D. Hager, H. Görls, U. S. Schubert, *Chem. Asian J.* **2011**, *6*, 2816–2824.
[22] T. M. McPhillips, S. E. McPhillips, H. J. Chiu, A. E. Cohen, A. M. Deacon, P. J. Ellis, E. Garman, A. Gonzalez, N. K. Sauter, R. P. Phizackerley, S. M. Soltis, P. Kuhn, *J. Synchrotron Radiat.* **2002**, *9*, 401–406.
[23] W. Kabsch, *J. Appl. Crystallogr.* **1993**, *26*, 795–800.
[24] G. M. Sheldrick, *Acta Crystallogr., Sect. A* **2008**, *64*, 112–122.

Received: September 26, 2014
Published Online: December 11, 2014

